The Possibilistic Correlation-Dependent Fusion Methods for Optical Detection

SHAHEERA RASHWAN
Knowledge-Based Systems and Robotics Department, Informatics Research Institute, Mubarak City for Scientific Research, Borg ElArab, Alexandria, Egypt
shaheerarashwan@lycos.com
http://www.mucsat.sci.eg/

Abstract: - Multi sensor fusion is an important component of applications for systems that use correlated data from multiple sensors to determine the state of a system. As the state of the system being monitored and many sensors are affected by the environmental conditions changing with time, the multi sensor fusion requires a correlation-dependent approach. The behavior of this approach should vary according to the correlation parameter. In this paper, we compare our possibilistic correlation-dependent fusion approach (PCDF) with the possiblistic combiner Dempster-Shafer. We focus in this paper on the mathematical background of this approach so that it can be used in many useful applications. We use time-series infrared images of landmines buried in different types of soil.
Key-Words: - Image Fusion, Correlation, T-Norm, Dempster Shafer, time-series images of buried mines.

1 Introduction

Multi image fusion has become an active field of research as more and more applications such as medical imaging, security, avionics, surveillance and night vision utilize multi sensor imaging arrays. Such arrays provide a wider spectral coverage and reliable information even in adverse environmental conditions at a price of a considerable increase in the amount of data. Image fusion deals with the data overload by combining visual information from multiple image signals into a single fused image.

Detection techniques for buried low-metal landmines that are in development can be grouped into three main categories: (i) sensors that 'see' an image of the landmine through scattering, (ii) sensors that detect anomalies at the surface or in the soil, and (iii) sensors that detect the landmine explosives or chemicals that are associated with the explosives. Most if not all of these sensors are affected to some degree by soil conditions.

There is a general agreement that no sensor can by itself be used to find landmines under all conditions. Data fusion techniques are used to combine the information from different sensors to increase the probability of detection and decrease the false-alarm rate.

Most work on data fusion for landmine detection has involved data fusion at the decision level [2]. If the performance of the individual sensors is strongly correlated, then the sensor fusion algorithm may also need the correlation coefficients.

As a practical matter, models of sensor performance do not seem to be accurate enough to directly provide this information. Given that soil properties can have a very large influence on the ROC curve associated with a particular sensor [15], we suggest incorporating information about the change in the soil properties conditions in the area under investigation into the data-fusion process.

In [12], L. Kuncheva et al. consider two main issues in designing cluster ensembles "separately": (1) the design of the individual "clusterers" so that they form potentially an accurate ensemble, and (2) the way the outputs of the clusterers are combined to obtain the final partition, called the *consensus* function.

In our new cluster ensemble methods (PCDF, Possibilistic Correlation-Dependent Fusion) [10, 11] the two issues are merged into a single design procedure, i.e., when one clusterer is added at a time and the overall fusion function is updated according to the correlation between the two images to be fused. It is seen that correlation between two consecutive MWIR images is related to the environmental changes (temperature, water content, texture, bulk density).

2 Fusion Techniques

Fusion techniques can be seen as a *discriminant* function, $F(\vec{c})$ in image confidence space defined in such a way that:

$F(\vec{c}) \geq t$ *assign* $\vec{c} \rightarrow$ Object of Interest

$F(\vec{c}) < t$ *assign* $\vec{c} \rightarrow$ Background

where $\vec{c} = (c_1, c_2, ..., c_R), c_i \in [0,1] \ \forall i \in [1, R]$ is an image output (confidence) vector with R the number of images and t the threshold. Image output vectors are defined only at locations where the images from co-registration and where image data is present.

The general layout of the image-fusion methods is shown in Figure 1. The input of each image-fusion method is a confidence level per grid cell.

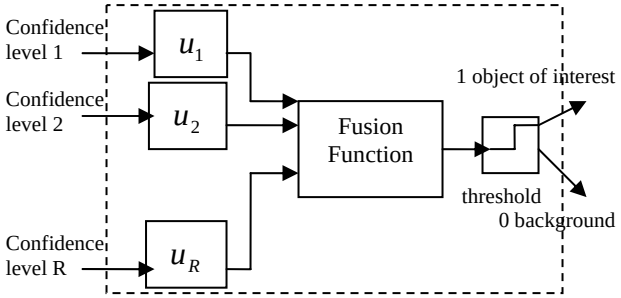

Figure .1. The generic image-fusion layout.

The output of the fusion process is one for detection and zero for no detection per grid cell. Each of the methods scales the influence of each of the images in a different way.

This mapping may remove the differences in definitions of the confidence levels. The mapped inputs are combined in a fusion function to acquire a single value per grid cell. The mapping functions and the fusion function are given in [1, 2, 3, 4]. In IR images, the mine has higher intensity than its surrounding this is how it can be detected.

3 The Dempster-Shafer Fusion Method

For application of the Dempster-Shafer theory to image fusion, three inputs per image are needed: the probability mass assigned to an object of interest $m(M)$, the probability mass assigned to background $m(\overline{M})$, and the unassigned probability mass $m(M \cup \overline{M})$. The sum of these masses always equals one, so there are only two *independent* masses ($m(M)$ and $m(\overline{M})$). The mass $m(M)$ represents a belief in an object of Interest, the mass $m(\overline{M})$ represents the belief in background, and the mass $m(M \cup \overline{M})$ reflects the uncertainty of the image. Each image produces one confidence level at each sample location, which must be mapped onto the three required probability masses. This is done by using the uncertainty as an optimization parameter.

The confidence levels for image i are mapped onto probability masses, using:

$$m_i(M) = (1-u_i)c_i \quad (1)$$

$$m_i(M \cup \overline{M}) = u_i \quad (2)$$

with u_i the mapping parameter and c_i the confidence level for image i . Frank Cremer et al.[1,2,3,4] use the Dempster-Shafer for combining only three sensors. As in time-series images, we can combine more than three images, we had to compute the general form for R images.The probability masses for image 1, 2,..,R are combined using Dempster's rule of combination:

$$m_{1,2,\ldots,R}(M) = (m_{1,2,\ldots,R-1}(M) + m_{1,2,\ldots,R-1}(M \cup \overline{M})) * m_R(M) + m_R(M \cup \overline{M}) * m_{1,2,\ldots,R-1}(M) \quad (3)$$

$$m_{1,2,\ldots,R}(M \cup \overline{M}) = \prod_{i=1}^{R} m_i(M \cup \overline{M}) \quad (4)$$

with $m_{1,2,\ldots,R}(M)$ the combined probability mass assigned to object of interest, and $m_{1,2,\ldots,R}(M \cup \overline{M})$ the combined uncertainty mass. The output of the Dempster-Shafer fusion function is given by the three combined probability mass assigned to an object of interest plus half the uncertainty:

$$F(\vec{c}) = m_{1,2,\ldots,R}(M) + \tfrac{1}{2} m_{1,2,\ldots,R}(M \cup \overline{M}) \quad (5)$$

From the previous, we conclude that Dempster-shafer belief functions are assigned to independent sources of evidence and is known as a special case of possibilisty theory where correlation = 0 [8] and hence, it is not expected from this theory to have a good behavior in applications of high correlation data such as landmine detection. In later sections, we will present our PCDF approach sensitive to correlation.

4 The Possibilistic Correlation-Dependent Fusion Methods

We propose a general method for the fusion process, which can be used with image outputs that may exhibit any kind of (positive, neutral, or negative) correlation with each other. Our method is based on the concept of Triangular Norms, a multi-valued logic generalization of the Boolean intersection operator. With the intersections of multiple decisions one needs to account for possible correlation among the sources, to avoid under- or over-estimates. Here we explicitly account for this by the proper selection of a T-norm operator. We combine the outputs of the images by the generalized intersection operator (T-norm) that better represents the possible correlation between the images. This approach performs better for correlated satellite images for environmental changes than the previous techniques [10-11].

The correlation affects the performance analysis [1]. The larger the correlation index, the larger the redundancy. In particular, the correlation index goes to zero if the individual incorrect answers are disjoint for all answers. In other words there is always at least one correct answer for any class.

The ρ correlation coefficient [6] gets larger as the number of wrong answers is the same for many answers. Let N^f be the number of experiments where all tools had a wrong answer, N_i^c be the number of experiments with combinations of correct and incorrect answers; c is the combination of correct and incorrect answers; n is the number of tools. The correlation coefficient is then

$$\rho = \frac{nN^f}{\sum_{i=1}^{2^n-2} N_i^c + nN^f} \quad (7)$$

N^f and N_i^c are computed using the correlation analysis matrix [5]. We have chosen this computation of correlation since N_i^c / N represents the environmental change factor. N represents the total number of experiments. The range of ρ here varies from 0 to 1 where $N^f = 0$ to $N_i^c = 0$. So, we exclude the Yager T-Norm family for the ρ out of range, refer to[16-17]. Let $\beta = N_i^c / N$, it is clear that when β is low, ρ is high and vice versa. The importance of β rely on its meaningful representation for the end-user of the optical device.

In I.Bloch[7], it was suggested to combine the information related to each class in a way which is adapted to the conflict between the sources concerning this class, as

$$\forall M \in image, \mu_i(M) = F[\mu_i^1(M), \mu_i^2(M), conflic(\mu_i^1, \mu_i^2)] \quad (8)$$

The conflict here refers to β.

In our work, we suggest a new decision-level fusion method based on possibilistic fusion based on T-Norm for a better representation of the correlation among images.

T-norm	Value of ρ	Correlation Type
T_D **Drastic Product**	$\rho = +\infty$	**Extreme case of positive correlation**
T_L **Lukasiewicz**	$\rho = 1$	**Partial case of positive correlation**
T_P **Product**	$\rho = 0$	**No correlation**
T_M **Minimum**	$\rho = -\infty$	**Extreme case of negative correlation**

Table 1. This table shows the value of correlation related to the corresponding basic form of T-Norm

In table 1, we present the relationship between the correlation and the four basic forms of T-Norm. Since the correlation degrades the performance fusion, then the T-Norm has its strongest value T_M minimum when the correlation has its weakest value $\rho = -\infty$ (extreme case of negative correlation) and its weakest value T_D Drastic Product when the correlation has its largest value $\rho = +\infty$ (extreme case of positive correlation). When the classifiers are uncorrelated, i.e. $\rho = 0$, this corresponds to the evidential independence in Dempster-Shafer. Hence, the corresponding T-norm will be the T_P Product. The T_L Lukasiewicz corresponds to an intermediate stage of positive correlation $\rho = 1$ (Partial case of positive correlation).

From the associativity of the T-norms, we can derive the associativity of the fusion by:

$$F(\vec{c}) = TNorm\,(TNorm\,(c_1, c_2), c_3) = TNorm\,((c_1, TNorm\,(c_2, c_3)) \quad (9)$$

with c_1, c_2, c_3 the confidence levels for three images and this equation (9) can be computed recursively for R images. For instance the operator $h(x, y, \alpha)$ is CIVB (Context Independent Variable Behavior) whose behavior depends on the value of α [7].

In our approach, we choose a suitable α to have a fusion technique sensitive to correlation.

1. *Generalized T-Norm Family:*
   - This family is increasing w.r.t. the parameter α
   - We choose α such that $\alpha = \rho$

$$TNorm(c_i, c_{i+1}) = \max[0, (c_i^{\alpha} + c_{i+1}^{\alpha} - 1)]^{1/\alpha}, \quad \alpha \neq 0 \quad \alpha \neq 1 \quad (10)$$

$$TNorm(c_i, c_{i+1}) = \begin{cases} \max[0, (c_i + c_{i+1} - 1)] & \alpha = 1 \\ c_i * c_{i+1} & \alpha = 0 \\ \text{otherwise} \end{cases} \quad (11)$$

2. *Schweizer-Sklar T-Norm Family:*

- This family is a decreasing family w.r.t. the parameter α
- We choose α such that $\alpha = 1-(\rho/\infty)$

$$TNorm(c_i, c_{i+1}) = \frac{c_i * c_{i+1}}{\max(c_i, c_{i+1}, \alpha)}, \quad \alpha \neq 0 \quad \alpha \neq 1 \quad (12)$$

otherwise

$$TNorm\ (c_i, c_{i+1}) = \begin{cases} c_i * c_{i+1} & \alpha = 1 \\ \min(c_i, c_{i+1}) & \alpha = 0 \end{cases} \quad (13)$$

3. Frank T-Norm Family:

- This family is decreasing family w.r.t the parameter α
- We choose α such that $\alpha = 1/(1-\rho)$

$$TNorm\ (c_i, c_{i+1}) = \log_{\alpha}[1 + \frac{(\alpha^{c_i} - 1)(\alpha^{c_{i+1}} - 1)}{\alpha - 1}]$$

$$, \quad \alpha \neq 0,1,+\infty \quad (14)$$

otherwise

$$TNorm(c_i, c_{i+1}) = \begin{cases} \max[0, (c_i + c_{i+1} - 1)] & \alpha = +\infty \\ c_i * c_{i+1} & \alpha = 1 \\ \min(c_i, c_{i+1}) & \alpha = 0 \end{cases}$$

(15)

4. *Hamacher T-Norm Family:*

- This family increasing w.r.t. the parameter α
- We choose α such that $\alpha = 1/(1-\rho)$

$$TNorm(c_i, c_{i+1}) = \frac{c_i * c_{i+1}}{\alpha + (1-\alpha)(c_i + c_{i+1} - c_i * c_{i+1})}, \quad (16)$$

$\alpha \neq +\infty \quad \alpha \neq 1$

otherwise

$$TNorm(c_i, c_{i+1}) = \begin{cases} \max[0, (c_i + c_{i+1} - 1)] & \alpha = +\infty \\ c_i * c_{i+1} & \alpha = 1 \end{cases}$$

(17)

5 Experiments on Real data

In the performance evaluation table, the accuracy is compared to the correlation between different images of environmental changes. The images are acquired from http://apl-database.jrc.it/Home/sigdata.htm/ for landmine MWIR images in a sand lane, gravel lane, mixture lane.

These data were collected at Meerdael (Belgium) minefields on 1st, 2nd and 3rd of April 1998 using mid-wave infrared cameras - AGEMA (3um-5um). These images are chosen to prove the efficiency of the algorithm and its usefulness in the landmine detection applications [9]. The accuracy here is defined by comparing the actual image with the fused image. The actual image here is the "best sensor" – the base image with the highest classification accuracy (minimum error by the clustering method used).

In order to create this comparison it is of extreme importance to have adequate simultaneous information on the detection rate over the entire diagram for the algorithm.

The data used for performance evaluation:

1. AGEMA MWIR image in a sand lane(referred to S1 row in table 2) acquired at date 01-04-1998 and times 21:34M and 22:04M
   Computed Correlation = 0.65631
2. AGEMA MWIR image in a sand lane(referred to S2 row in table 2) acquired at date 01-04-1998 and times 13:08M and 13:59M
   Computed Correlation = 1
3. AGEMA MWIR image in a gravel lane (referred to G row in table 2) acquired at date 02-04-1998 and times 20:49M and 21:23M
   Computed Correlation = 0.91762
4. AGEMA MWIR image in a mixture lane (referred to M row in table 2) acquired at date 03-04-1998 and times 21:19M and 21:48M
   Computed Correlation = 0.94982

DATA	Accuracy of Techniques				
	DS	**G**	**S-S**	**F**	**H**
S1	-----	0.93757	0.93757	0.93757	0.93757
S2	0.8956	0.5245	0.5245	0.5245	0.5245
G	0.89795	0.92569	0.92569	0.92569	0.92569
M	0.9317	0.95358	0.95358	0.95358	0.95358

Table2. Accuracy gained by the Dempster Shafer technique and the different forms of the PCDF approach. The points (----) means that the algorithm fails to detect any of the object of interest.

The following figures show the output fused images using Dempster-Shafer and the PCDF (the four T-Norm CIVB forms gave appropriate results here)

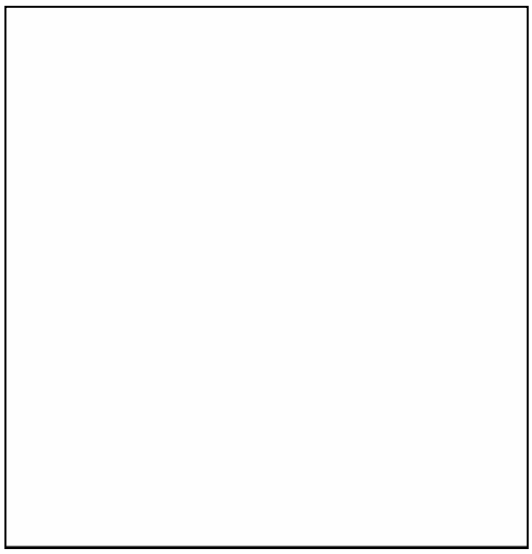

Figure 2.The output fused image using Dempster-Shafer (sand lane S1)

Figure 3.The output fused image using the PCDF (sand lane S1)

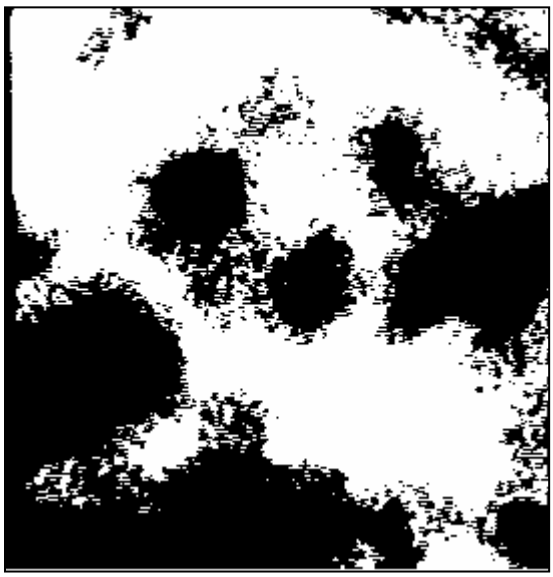

Figure 4.The output fused image using the Dempster-Shafer (sand lane S2)

Figure 5.The output fused image using the PCDF (sand lane S2)

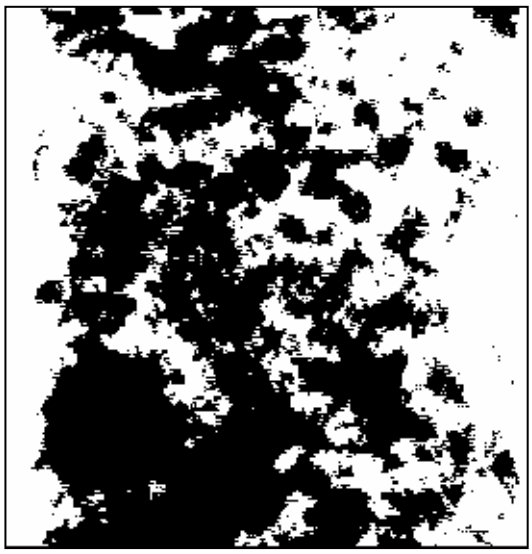

Figure 6.The output fused image using the Dempster Shafer (gravel lane)

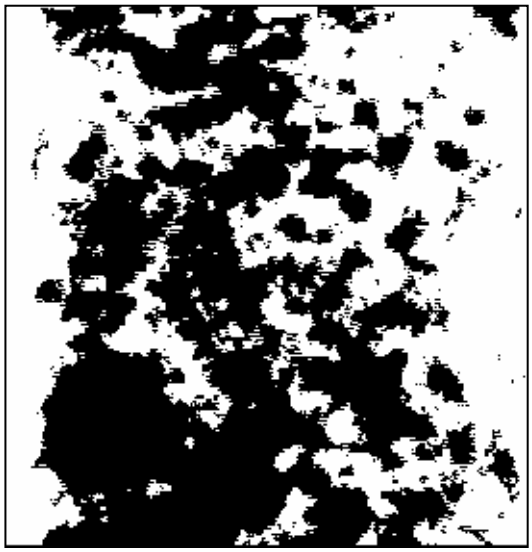

Figure 7.The output fused image using the PCDF (gravel lane)

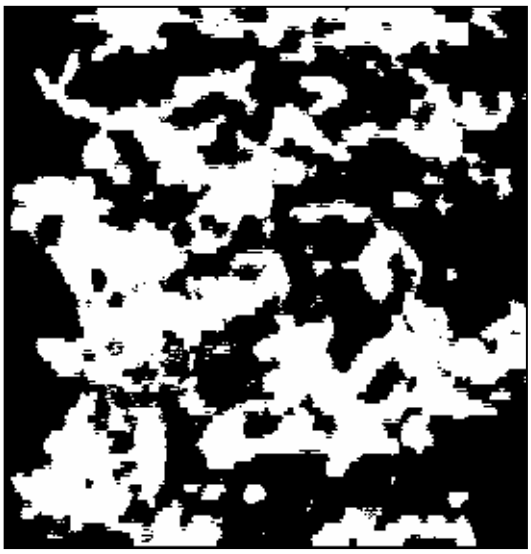

Figure 8.The output fused image using the Dempster Shafer (mixture lane)

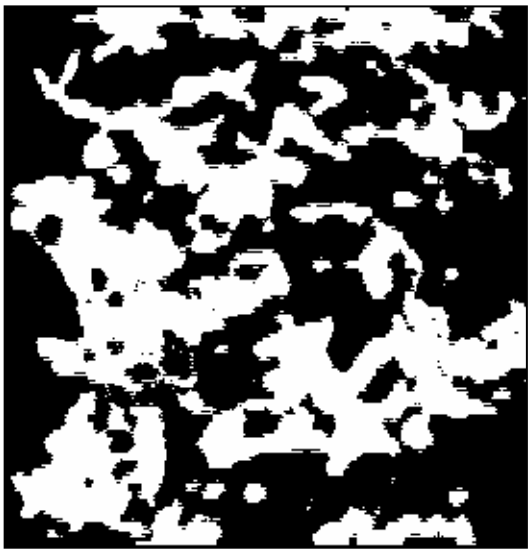

Figure 9.The output fused image using the PCDF (mixture lane)

5 Conclusions

We have proposed an approach based on possibility theory in this paper. The approach is based on computing the correlation among different images taken at different times to study the change of the environment and use it as a parameter in four T-Norm Correlation-Dependent fusion techniques to handle the problem of high correlation by introducing the correlation parameter in the fusion process. The approach is better evaluated perceptually. The thermal

signatures in a sand lane give better results than in gravel or in mixture lane.

6 Future Works

In this paper, we presented two types of T-Norm families which are increasing and decreasing w.r.t. the parameter α families. The behavior of the PCDF was the same when applied to time-series images of large changes of the environment (long periods of time proportional to the landscape acquired) while time-series images of small changes of the environment (short periods of time proportional to the landscape acquired)[11], the difference between both types of families is distinguished.

For future work, we will focus on the comparison between decreasing and increasing T-Norms families and the choice of the suitable form of the PCDF Method in the application to a particular problem. An investigation about a performance evaluation method to compare different techniques is also required. To be noted, time-series images are *only* used for optics detecting of an unchanged object in a changeable environment (different light systems affect the output of high-sensitivity optic devices). In this case, we compensate the non-existence of the suitable wavelength or spectrum by fusing more than one image in consecutive times.

7 Acknowledgements

This project is supported by Informatics Research Institute, Mubarak City for Scientific research, Alexandria, Egypt-Research joint project Egypt-China under the supervision of Prof. Dr. Walaa Sheta

References:

[1]Piet B.W. Schwering, Brian A. Baertlein, Sebastiaan P. van den Broek, Frank Cremer, "Evaluation methodologies for comparison of fusion algorithms in land mine detection", in Proc. SPIE Vol. 4742, Detection and Remediation Technologies for Mines and Minelike Targets VII , Orlando FL, USA, Apr. 2002

[2] F.Cremer, K.Schutte, J.G.M. Schavemaker, E. den Breejen, "A comparison of decision-level sensor-fusion methods for anti-personnel landmine detection", in Information Fusion 2, pp.187-208, 2001

[3] F.Cremer, K.Schutte, J.G.M. Schavemaker, E. den Breejen, "Towards an operational sensor-fusion system for anti-personnel landmine detection", in Proc. SPIE Vol. 4038, Detection and Remediation Technologies for Mines and Minelike Targets V , Orlando FL, USA, Apr. 2000

[4] Hao Yin, ElSayed A. Orady, Yubao Chen, Chia-hao Chang, "A practical measure of the uncertainty level in a data set", in International Journal of Science & Technology, Vol.14, 2003

[5] Kai Goebel, Weizhong Yan, "Choosing Classifiers for Decision Fusion", Proceedings of the Seventh International Conference on Information Fusion, vol. I, pp. 563-568, 2004.

[6] K. Goebel, W. Yan, and W. Cheetham, "A method to calculate classifier correlation for Decision Fusion" Proceedings of IDC 2002, Adelaide, 11-13 February, 2002., pp. 135-140, 2002.

[7]Isabelle Bloch, "Information Combination Operators for data fusion: A comparative review with classification", in IEEE Trans. on Systems, Man, and Cybernetics-Part A: Systems and Humans, Vol.26, NO. 1, pp.52-67, January 1996.

[8] P. Bonissone, K. Goebel, W. Yan, "Classifier fusion using T-norms" Lecture Notes in Computer Science: Proceeding of the Fifth International Workshop on Classifier Fusion, pp. 154-163, 2004.

[9] Igor V.Maslov, Izidor Gertner, "Multi-sensor fusion: an Evolutionary algorithm approach", Information Fusion 7(2006), pp 304-340

[10]S.Rashwan, M.A.Ismail, S.Fouad, "Possibilistic Fusion for Landcover Mapping using Correlated Satellite Imagery for Environmental Change", WSEAS proceedings of the 5th Int. Conf. on Computational Intelligence, Man-Machine systems And Cybernetics (CIMMACS'06) , pp.29-33, November 2006.

[11]S.Rashwan, M.A.Ismail, S.Fouad, "Landcover Mapping using Triangular-Norms", WSEAS transactions on computers research, Issue 1, Volume 1, pp.19-24, November 2006

[12] Kuncheva L.I., S.T. Hadjitodorov, L.P. Todorova, "Experimental comparison of cluster ensemble methods", Proc FUSION 2006

[13] S.Rashwan, M.A.Ismail, S.Fouad, "Detection of buried landmines in MWIR Time-series Images using the Possibilitic Correlation-Dependent Fusion Methods", WSEAS transactions on Systems and Control, Issue 2, Volume 2, pp 218-223, February 2007

[14] S.Rashwan, M.A.Ismail, S.Fouad, "Mine Detection using Possibilistic Fusion of consecutive Infrared Images", WSEAS transactions on Signal Processing, Issue 12, Volume 2, pp 1579-1586, December 2006

[15] Remke L. Van Dam, Brian Borchers and Jan M. H. Hendrickx," Strength of landmine signatures under different soil conditions: implications for sensor fusion" International Journal of Systems Science, pp 1-15, 2005
[16]Erich Peter Klement, Radko Mesiar, Endre Pap," Triangular norms. Position paper II: general constructions and parameterized families" Fuzzy Sets and Systems 145 (2004) pp411–438
[17]Erich Peter Klement, Radko Mesiar, Endre Pap," Position paper I: basic analytical and algebraic properties" Fuzzy Sets and Systems 143 (2004) 5–26